PHYSICAL REVIEW E **84**, 051204 (2011)

Anomalous change in the dynamics of a supercritical fluid

Sungho Han

Department of Physics and Astronomy, University of California, Irvine, California 92697, USA

(Received 7 July 2011; revised manuscript received 27 October 2011; published 15 November 2011)

We perform molecular dynamics simulations to investigate dynamical properties of a supercritical Lennard-Jones fluid. We find that in the supercritical region there is a short-ranged deviation in dynamic character. We further find that this anomalous change is associated with the presence of the Widom line, the locus of specific heat maxima, of the liquid-vapor phase transition. The salient change in dynamics is consistent with a crossover in the correlation of the diffusion coefficient with the excess entropy. Our results lead to an interpretation that, even though a supercritical fluid excludes a singularity, its dynamical properties can be significantly affected by the existence of thermodynamic response maxima.

DOI: 10.1103/PhysRevE.84.051204 PACS number(s): 61.20.Ja, 64.70.F−, 61.20.Ne, 64.60.Bd

A special thermodynamic line known as the Widom line, the locus of specific heat maxima, exists in continuity with a coexistence line of two phases beyond a critical point [1]. Generally, phase transitions in liquids, such as solid-liquid and liquid-vapor transitions, have been of wide interest [2–4]. Recently, water researches have initiated extensive studies of the Widom line due to the hypothesized liquid-liquid second critical point in supercooled water [1,5–8]. Since a direct experimental search for the liquid-liquid critical point is prohibited by spontaneous crystallization, and since the Widom line provides alternative evidence of the critical point, many experimental and computational studies have focused on the Widom line of the liquid-liquid transition [1,5,6,9,10].

Many studies of supercooled water found that the Widom line of the liquid-liquid transition crucially affects dynamic quantities as well as static quantities [1,5,6,8–11]. Inelastic neutron scattering experiments of confined water have found that there is a fragile-to-strong dynamic crossover of the structural relaxation time in the supercooled region [9,12]. Experimental and computational studies have further revealed that the temperature of the dynamic crossover indeed coincides with the Widom temperature [1,5,6,9]. The fragile-to-strong transition in water has been first proposed from evidence that water changes dynamic character from a fragile liquid at temperatures above 236 K to a strong liquid near 136 K [13]. Similarly, simulation studies for supercooled silicon have found a change in dynamic character associated with the first-order liquid-liquid phase transition between a fragile (high-density) liquid and a strong (low-density) liquid [14].

The Widom line also exists in the supercritical region beyond the liquid-vapor critical point. Compared to the Widom line of the liquid-liquid transition, the Widom line of the liquid-vapor transition has not been extensively studied so far. Recently, inelastic x-ray scattering studies of argon revealed the important role of the Widom line of the liquid-vapor transition as a subtle boundary between liquidlike and vaporlike behaviors in the supercritical region [15]. This experimental result suggests that the presence of the Widom line may significantly affect the thermodynamic and dynamical properties of supercritical fluids. However, the effect of the Widom line on the dynamics of the supercritical fluid remains unknown. Of particular interest is whether the presence of the Widom line has a universal effect on dynamics of fluids. In this paper, we investigate how dynamics of a supercritical Lennard-Jones (LJ) fluid is affected by the presence of the Widom line of the liquid-vapor transition and further examine if there is a universal effect on dynamics by the Widom lines of both the liquid-liquid and liquid-vapor transitions.

We carried out extensive molecular dynamics (MD) simulations of $N = 1728$ LJ fluids in NPT (N: the number of particles; P: pressure; and T: temperature) ensembles. LJ particles interact with each other through the LJ interparticle potential defined as

$$U_{\rm LJ}(r) = 4\epsilon\left[\left(\frac{\sigma}{r}\right)^{12} - \left(\frac{\sigma}{r}\right)^{6}\right]. \quad (1)$$

Here the LJ parameters ϵ and σ represent energy and length scales, respectively, and r is the distance between two particles. We truncated the LJ interparticle potential at a cutoff radius $r_{\rm c} = 4.0\sigma$, and then shifted it to make the potential and force continuous at $r = r_{\rm c}$ [16]. We used the reduced MD dimensionless units (denoted by a superscript $*$) using appropriate combinations of energy scale ϵ, length scale σ, mass m, and the Boltzmann's constant $k_{\rm B}$ throughout this work [16]. We implemented the Berendsen thermostat and barostat to keep the temperature and pressure constant [17]. We used periodic boundary conditions in all x, y, and z directions.

First, we calculate the local structure of a LJ fluid. Note that in our calculation the liquid-vapor critical point is located at $T^*_{\rm c} \simeq 1.305$ and $P^*_{\rm c} \simeq 0.16$ (Fig. 1). In Fig. 2, we present the radial distribution function $g(r^*)$ as a function of distance r^* for different T^* at constant $P^* = 0.20$ ($> P^*_{\rm c}$). The local structure obtained from $g(r^*)$ does not show a significant change with crossing the Widom line. As T^* increases, the peaks in $g(r^*)$ gradually decrease. Whereas crossing the Widom line of the liquid-liquid transition in supercooled water induces a significant change of the structure of water [11], the local structure of the supercritical LJ fluid does not exhibit a significant change with crossing the Widom line. The difference may come from the fact that two liquids are structurally different and two Widom lines are located in a different temperature regime. It is of interest to mention that the third peak, although it is small, appearing in $g(r)$ for $T^* < T^*_{\rm w}$ (the Widom temperature) disappears for $T^* > T^*_{\rm w}$.

To examine if the Widom line affects dynamical properties in the supercritical region, we calculate the diffusion coefficient D via the Einstein relation, $\lim_{t\to\infty}\langle[\Delta r(t)]^2\rangle = 2dDt$,

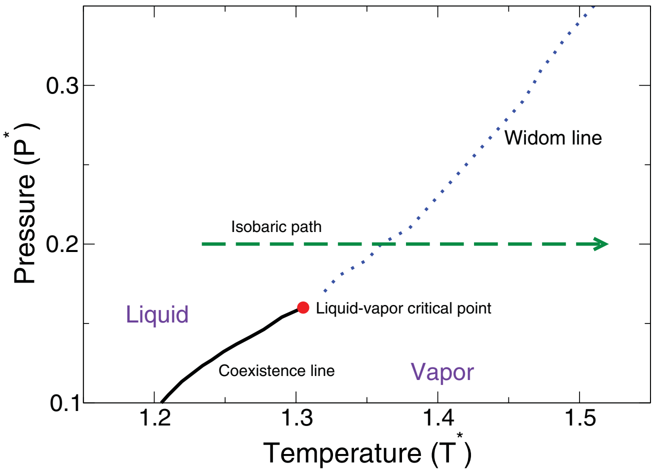

FIG. 1. (Color online) Phase diagram of the LJ fluid in the temperature-pressure ($T^* - P^*$) plane. A black solid line is the liquid-vapor coexistence line. A red circle is the liquid-vapor critical point. Blue dots represent the locus of the isobaric specific heat maxima. A green dash line is the isobaric path ($P^* = 0.20$) we used in this study. All data are taken from our simulation results.

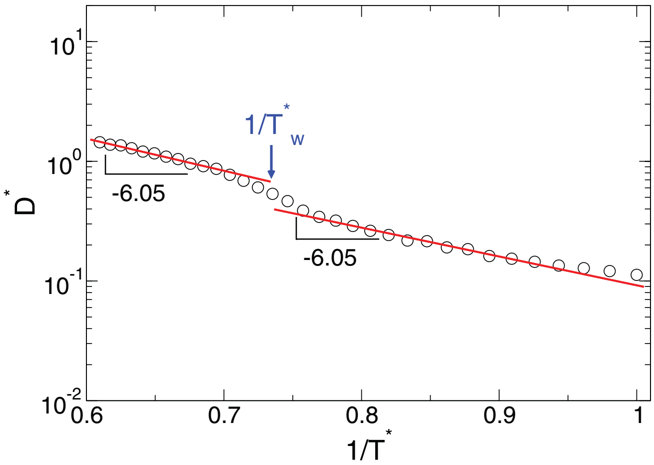

FIG. 3. (Color online) Shown in a semilog plot is the diffusion coefficient D^* as a function of $1/T^*$ at pressure $P^* = 0.20\,(>P_c^*)$. D^* at high temperatures can be well fit by an Arrhenius form of temperature dependence, $D^* \propto \exp[-E_A^*/T^*]$. Around the Widom line (denoted by an arrow), as T^* varies, D^* rapidly changes by deviating from the Arrhenius fit. The slopes of the Arrhenius fit (E_A^*) for $T^* > T_w^*$ and $T^* < T_w^*$ show the same values ($E_A^* \simeq 6.05$).

where d is dimensionality [4,18]. In Fig. 3, we present D^* as a function of $1/T^*$ at constant $P^* = 0.20\,(>P_c^*)$. At high T^*, D^* can be well fit by an Arrhenius form of temperature dependence, given by $D^* \propto \exp[-E_A^*/T^*]$, and it slightly deviates from the Arrhenius fit at low T^*. Note that the difference between an Arrhenius ($\sim\exp[-E_A/k_B T]$) and a non-Arrhenius temperature dependence represented by the Vogel-Fulcher-Tammann function ($\sim\exp[-E_A/k_B(T - T_0)]$) becomes negligible for high temperatures of $T \gg T_0$. Interestingly, we find an anomalous behavior of D^* around the Widom temperature T_w^*, as shown in Fig. 3. As T^* approaches T_w^* from below, D^* saliently, rather than steadily, increases by deviating from the Arrhenius fit, and in the reverse direction D^* decreases in the same way as D^* increases. However, crossing the Widom line does not modify temperature dependence form of D^*. The E_A in the Arrhenius fit, interpreted as the activation energy for self-diffusion, shows the same value ($E_A^* \simeq 6.05$) before and after crossing the Widom line. The significant change in $\ln D^*$ with respect to $1/T^*$ occurs only near the Widom line. Since this anomalous change is represented by a bending of a straight line in the plot of $\ln D$ versus $1/T$, we call this anomalous change of D associated with the Widom line *a dynamic bend*, similar to the dynamic crossover [1,5,9]. The existence of the dynamic bend indicates that although a supercritical fluid excludes a singularity, its dynamics is significantly affected by the presence of the Widom line. Here we might need to address a comparison between the dynamic bend and the critical slowing down [19]. Approaching a critical point, the relaxation time τ of a system dramatically increases in the form of $\tau \sim |T - T_c|^{-\zeta}$, known as the critical slowing down. The dynamic bend shows a rapid increase or decrease of D depending on heating or cooling, whereas for the critical slowing down D only decreases drastically as T approaches T_c.

For various liquids, there have been many efforts to find a connection between the translational self-diffusion and the excess entropy [20–25]. The (intensive) excess entropy s^{ex} is defined as

$$s^{ex} \equiv s - s_{id}, \tag{2}$$

the difference between the total entropy s and the entropy of an ideal gas $s_{id}\,[\equiv -k_B \ln\rho + w(T)]$, where ρ is density and $w(T)$ is a temperature-dependent constant [22,24,25]. Note that a more negative value of s^{ex} represents more ordered structure. s^{ex} can be estimated from the two-body contribution on the excess entropy $s_{(2)}^{ex}$ in an expansion of s^{ex} with respect

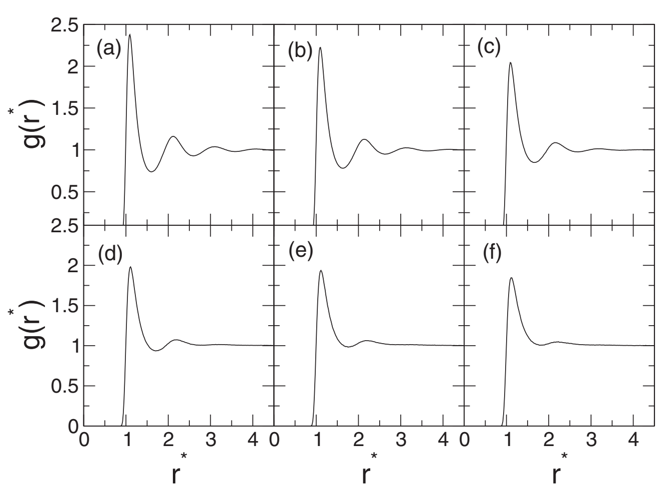

FIG. 2. The radial distribution function $g(r^*)$ as a function of distance r^* at pressure $P^* = 0.20\,(>P_c^* \simeq 0.16)$ and six different temperatures (a) $T^* = 1.02$, (b) $T^* = 1.12$, (c) $T^* = 1.26$, (d) $T^* = 1.36$ ($\approx T_w^*$), (e) $T^* = 1.44$, and (f) $T^* = 1.58$. As T^* increases along the isobaric path, $g(r^*)$ shows that the peaks gradually decrease.

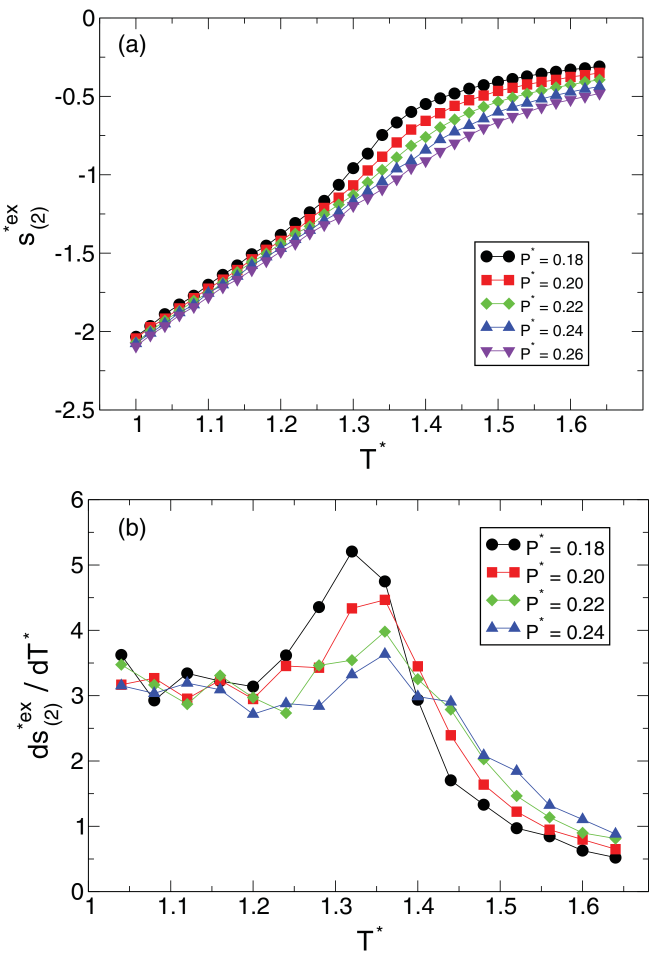

FIG. 4. (Color online) (a) The two-body excess entropy $s_{(2)}^{*\mathrm{ex}}$ and (b) the two-body excess entropy change $ds_{(2)}^{*\mathrm{ex}}/dT^*$ as a function of temperature T^* for different pressures in the supercritical region. $ds_{(2)}^{*\mathrm{ex}}/dT^*$ shows the maximum at the Widom temperature $T_{\mathrm{w}}^*(P^*)$.

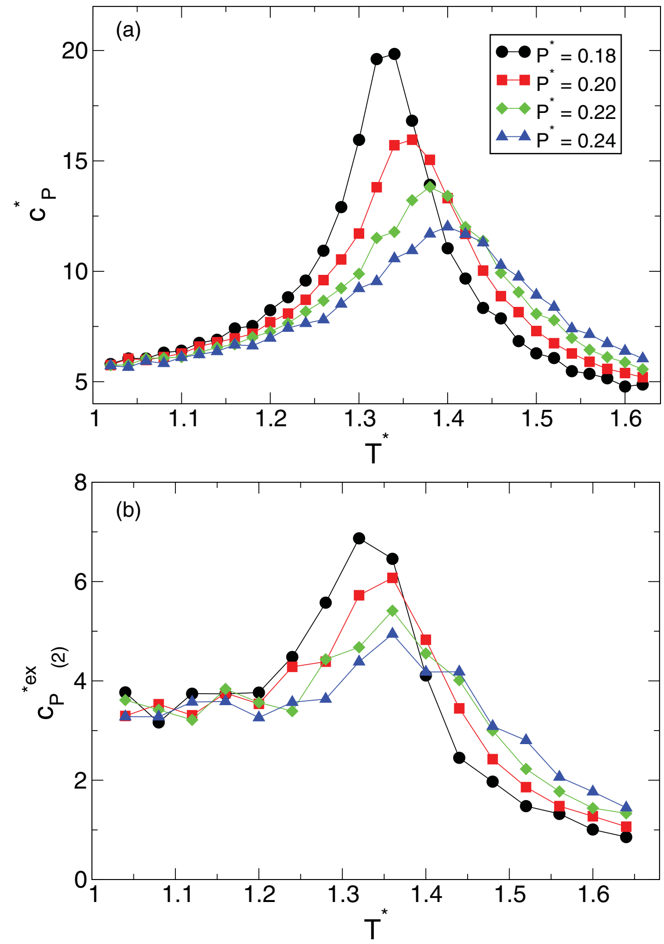

FIG. 5. (Color online) (a) The isobaric specific heat c_P^* and (b) the two-body excess isobaric specific heat $c_{P(2)}^{*\mathrm{ex}}$ [$\equiv T^*(ds_{(2)}^{*\mathrm{ex}}/dT^*)_{P^*}$] as a function of temperature T^* for different pressures in the supercritical region. Both c_P^* and $c_{P(2)}^{*\mathrm{ex}}$ show the maximum at the Widom temperature $T_{\mathrm{w}}^*(P^*)$.

to the radial distribution function $g(r)$ as follows [26]:

$$s_{(2)}^{\mathrm{ex}} \equiv -2\pi\rho k_{\mathrm{B}} \int \{g(r)\ln[g(r)] - [g(r)-1]\}r^2 dr. \quad (3)$$

Since $s_{(2)}^{\mathrm{ex}}$ is related to $g(r)$, it can be used for an alternative measure of the translational structure of the system. The two-body excess entropy $s_{(2)}^{\mathrm{ex}}$ gives a reasonable estimate of the excess entropy s^{ex} for various systems [22,26]. For example, $s_{(2)}^{\mathrm{ex}}$ for LJ systems is approximately between 85% and 95% of s^{ex} over a fairly wide range of densities [26]. $s_{(2)}^{\mathrm{ex}}$ has been used to represent the cascade regions of structural, dynamic and thermodynamic anomalies of water in the phase diagrams [22,24,25].

Next we investigate a connection between the dynamic bend and the excess entropy $s_{(2)}^{\mathrm{ex}}$. Using the results of $g(r^*)$ and Eq. (3), we calculate the two-body excess entropy $s_{(2)}^{*\mathrm{ex}}$ as a function of T^* at constant $P^* = 0.2$ ($> P_{\mathrm{c}}^*$). At higher T^*, $s_{(2)}^{*\mathrm{ex}}$ becomes less negative, indicating that the structure becomes more disordered. In Fig. 4(a), we find an interesting behavior of $s_{(2)}^{*\mathrm{ex}}$ associated with the Widom line. As T^* approaches T_{w}^*, $s_{(2)}^{*\mathrm{ex}}$ rapidly changes, and this change becomes weaker as P^* is away from P_{c}^*. One can clearly see this behavior of $s_{(2)}^{*\mathrm{ex}}$ on the Widom line from the calculation of the two-body excess entropy change $ds_{(2)}^{*\mathrm{ex}}/dT^*$. In Fig. 4(b), the calculation of $ds_{(2)}^{*\mathrm{ex}}/dT^*$ shows a maximum at $T^* = T_{\mathrm{w}}^*$, and the maximum value becomes smaller with increasing P^*.

Since the excess isobaric specific heat c_P^{ex} is directly related to ds^{ex}/dT, we further calculate the two-body excess isobaric specific heat $c_{P(2)}^{\mathrm{ex}} = T(ds_{(2)}^{\mathrm{ex}}/dT)_P$, and compare it with the (normal) isobaric specific heat $c_P = (1/N)(dH/dT)_P$, where H is the enthalpy. In Fig. 5, we present c_P^* and $c_{P(2)}^{*\mathrm{ex}}$ as a function of T^*. Both isobaric specific heats exhibit a maximum value at $T^* = T_{\mathrm{w}}^*$, and the peaks in both c_P^* and $c_{P(2)}^{*\mathrm{ex}}$ decrease with increasing P^*. It suggests that the calculations of s^{ex}, an order parameter of the translational structure, can provide a good probe of the Widom line of the liquid-vapor transition rather than the calculation of $g(r)$, an indicator of the local structure.

To find a connection between the dynamic bend and excess entropy, we examine D in terms of $s_{(2)}^{\mathrm{ex}}$. For supercooled liquids, Adam-Gibbs theory offers a description between the diffusion coefficient D and the configurational entropy S_{conf}

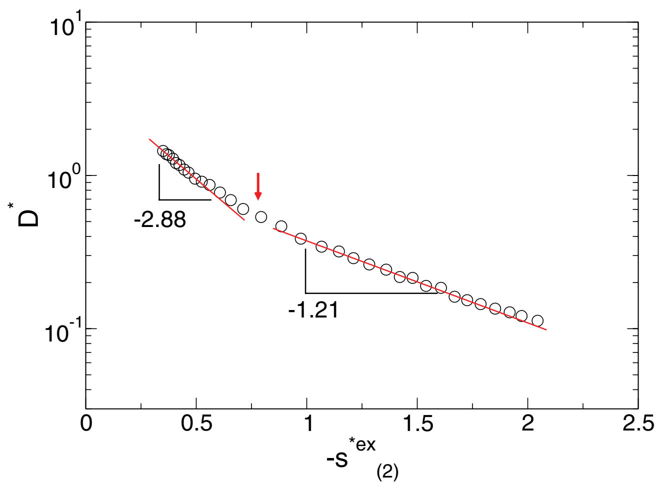

FIG. 6. (Color online) Shown in a semilog plot is the diffusion coefficient D^* versus the negative of the two-body excess entropy $-s^{*\mathrm{ex}}_{(2)}$ at $P^* = 0.20$ $(>P^*_c)$. It shows a crossover in the linear relationship between $\ln D$ and $s^{\mathrm{ex}}_{(2)}$, given by $D \propto \exp[Bs^{\mathrm{ex}}_{(2)}]$. The parameter B is 2.88 at high temperature and 1.21 at low temperature. The arrow denotes the location of the Widom line.

near the glass transition [27,28], given by

$$D \propto \exp\left[-\frac{A}{T\,S_{\mathrm{conf}}}\right], \tag{4}$$

where A is a temperature-independent parameter. Another description between D and $s^{\mathrm{ex}}_{(2)}$ has been introduced in various liquid systems [20,21], given by

$$D \propto \exp\left[Bs^{\mathrm{ex}}_{(2)}\right], \tag{5}$$

where B is a temperature-independent parameter. Whereas Eq. (4) provides a connection between the dynamics and the structure near the glass transition [27,28], Eq. (5) describes the whole liquid dynamics associated with the liquid structure [23–25]. The linear relationship between $1/(T\,S_{\mathrm{conf}})$ and $s^{\mathrm{ex}}_{(2)}$ in the supercooled region has been shown in computational studies of a core-softened fluid [23].

In Fig. 6, we present the diffusion coefficient D^* as a function of the negative of the two-body excess entropy $-s^{*\mathrm{ex}}_{(2)}$. As shown in Fig. 6, $\ln D^*$ shows a linear relationship with $-s^{*\mathrm{ex}}_{(2)}$. Interestingly, we find two different linear relationships between $\ln D^*$ and $-s^{*\mathrm{ex}}_{(2)}$ depending on T^*. The crossover in the linear relationship occurs around the Widom temperature T^*_{w}. The parameter B in Eq. (5) for high temperature (low $-s^{\mathrm{ex}}_{(2)}$) is 2.88, whereas B for low temperature (high $-s^{\mathrm{ex}}_{(2)}$) is 1.21. Note that the crossover in the linear relationship between $\ln D$ and $-s^{\mathrm{ex}}_{(2)}$ has been also found for hard sphere and square-well fluids in association with the onset of the breakdown of the Stokes-Einstein relation [24]. For supercooled water, the onset of the breakdown of the Stokes-Einstein relation is related to the Widom line of the liquid-liquid transition [6]. Since the relation between $\ln D$ and s^{ex} represents the correlation between the self-diffusivity and the structure, the crossover in the linear relationship between $\ln D$ and s^{ex} indicates a change in the correlation between the translational diffusion and the translational structural order. Our results of Figs. 3 and 6 show the possible connection between the dynamic bend and the crossover in the linear relationship between $\ln D$ and s^{ex}. They further imply that the dynamic bend originates from the rapid change in the correlation between the self-diffusion and translational order on the Widom line.

Our finding of the dynamic bend in the supercritical region leads to an important interpretation that the dynamical properties can be universally affected by the presence of the Widom line, as seen in both the dynamic crossover and the dynamic bend. Thus wherever one finds the Widom line, one can expect a change in dynamics of fluids, in association with its existence. However, it seems that there is a difference between the dynamic bend and the dynamic crossover due to the thermal effect and the structure difference of fluids. The dynamic crossover shows a sharp change in dynamic character between an Arrhenius fit and a non-Arrhenius fit of D at $T = T_{\mathrm{w}}$ [1,9,10,29]. The dynamic bend we found here does not exhibit the sharp change in the temperature dependence of D. Our finding will shed light on the full understanding of dynamical properties of fluids in the supercritical region. Whereas the dynamic crossover is restricted to the tetrahedral liquids, our results provide a high level of generality for understanding dynamics of fluids.

I thank John A. Brunelle, Moo Young Choi, Jaegil Kim, Pradeep Kumar, Albert Libchaber, H. Eugene Stanley, and Clare C. Yu for helpful discussions and critical comments.

[1] L. Xu, P. Kumar, S. V. Buldyrev, S.-H. Chen, P. H. Poole, F. Sciortino, and H. E. Stanley, Proc. Natl. Acad. Sci. USA **102**, 16558 (2005).
[2] B. Smit, J. Chem. Phys. **96**, 8639 (1992).
[3] N. B. Wilding, Phys. Rev. E **52**, 602 (1995).
[4] S. Han, M. Y. Choi, P. Kumar, and H. E. Stanley, Nat. Phys. **6**, 685 (2010).
[5] P. Kumar, Z. Yan, L. Xu, M. G. Mazza, S. V. Buldyrev, S.-H. Chen, S. Sastry, and H. E. Stanley, Phys. Rev. Lett. **97**, 177802 (2006).
[6] P. Kumar, S. V. Buldyrev, S. R. Becker, P. H. Poole, F. W. Starr, and H. E. Stanley, Proc. Natl. Acad. Sci. USA **104**, 9575 (2007).
[7] P. H. Poole, F. Sciortino, U. Essmann, and H. E. Stanley, Nature (London) **360**, 324 (1992).
[8] K. Stokely, M. G. Mazza, H. E. Stanley, and G. Franzese, Proc. Natl. Acad. Sci. USA **107**, 1301 (2010).
[9] L. Liu, S.-H. Chen, A. Faraone, C.-W. Yen, and C.-Y. Mou, Phys. Rev. Lett. **95**, 117802 (2005).
[10] F. Mallamace, C. Corsaro, M. Broccio, C. Branca, N. González-Segredo, J. Spooren, S.-H. Chen, and H. E. Stanley, Proc. Natl. Acad. Sci. USA **105**, 12725 (2008).
[11] L. Xu, F. Mallamace, Z. Yan, F. W. Starr, S. V. Buldyrev, and H. E. Stanley, Nat. Phys. **5**, 565 (2009).
[12] S.-H. Chen, L. Liu, E. Fratini, P. Baglioni, A. Faraone, and E. Mamontov, Proc. Natl. Acad. Sci. USA **103**, 9012 (2006).

[13] K. Ito, C. T. Moynihan, and C. A. Angell, Nature (London) **398**, 492 (1999).
[14] S. Sastry and C. A. Angell, Nat. Mater. **2**, 739 (2003).
[15] G. G. Simeoni, T. Bryk, F. A. Gorelli, M. Krisch, G. Ruocco, M. Santoro, and T. Scopigno, Nat. Phys. **6**, 503 (2010).
[16] D. C. Rapaport, *The Art of Molecular Dynamics Simulation* (Cambridge University Press, Cambridge, England, 2004).
[17] H. J. C. Berendsen, J. P. M. Postma, W. F. van Gunsteren, A. DiNola, and J. R. Haak, J. Chem. Phys. **81**, 3684 (1984).
[18] S. Han, P. Kumar, and H. E. Stanley, Phys. Rev. E **77**, 030201 (2008).
[19] H. E. Stanley, *Introduction to Phase Transitions and Critical Phenomena* (Oxford University Press, New York, 1971).
[20] M. Dzugutov, Nature (London) **381**, 137 (1996).
[21] Y. Rozenfeld, J. Phys.: Condens. Matter **11**, 5415 (1999).
[22] J. R. Errington, T. M. Truskett, and J. Mittal, J. Chem. Phys. **125**, 244502 (2006).
[23] J. Mittal, J. R. Errington, and T. M. Truskett, J. Chem. Phys. **125**, 076102 (2006).
[24] W. P. Krekelberg, J. Mittal, V. Ganesan, and T. M. Truskett, J. Chem. Phys. **127**, 044502 (2007).
[25] Z. Yan, S. V. Buldyrev, and H. E. Stanley, Phys. Rev. E **78**, 051201 (2008).
[26] A. Baranyai and D. J. Evans, Phys. Rev. A **40**, 3817 (1989).
[27] G. Adam and J. H. Gibbs, J. Chem. Phys. **43**, 139 (1965).
[28] P. G. Debenedetti and F. H. Stillinger, Nature (London) **410**, 259 (2001).
[29] P. Gallo, M. Rovere, and S.-H. Chen, J. Phys. Chem. Lett. **1**, 729 (2010).